Finite Element Modelling Of Surface Stresses In Coatings Under Single Particle Impact

Ashutosh Dubey , Francis John
Department of Mechanical Engineering and Applied Mechanics
Sam Higginbottom Institute of Agriculture, Technology and Sciences
Allahabad, U.P. INDIA

Abstract - In the present work finite element model was developed to investigate tensile stresses in the surface of coatings under single particle impact, simulating particulate erosion conditions. Modelling was done using ABAQUS/ Explicit Student Edition 6.5-3. Erosion resistant ability of coating was measured in terms of peak value of surface stress (tensile stress) in the coating. Lower the peak value of tensile stress better is the erosion resistant of the coating. Nine different coating architectures were analysed with different layer thickness and material properties. It may be suggested that the top layer of coating should be thin and bond layer should be thick to minimize tensile stress on coating surface which, in turn, improves erosion resistance ability of coating. It is also suggested to keep lesser value of young's modulus of coating to minimize tensile stress on surface thus improving its erosion resistance.

Keywords: Tensile stress; Radial stress distributions; Finite element method; coating thickness; Young's modulus; Modelling; Simulation.

1. Introduction

Erosive wear is defined as "Material damage caused by the attack of particles entrained in a fluid system impacting the surface at high speed" [1]. Solid particle erosion is a serious problem in gas turbines, rocket nozzles, cyclone separators, valves, pumps and boiler tubes. Also, it causes troubles in steam and jet turbines, pipelines used in slurry transportation of matter, and fluidized bed system [2]. Variables affecting the erosion process are particle velocity, particle size and angle of impact, particle shape, and particle density. Also, material property, its young's modulus, Poisson's ratio and failure behaviour also affects the erosion process [3].

There are many extensive reviews on this subject, such as those by Hutchings [4], Finnie [5], Bitter [6], and Sundarajan [7] just to name a few.

Objective of the present work is to find optimum coating architecture to maximize the reduction in the surface tensile stress generated in the coating under single particle impact. 3-D model of the system is developed. Four types of material (substrate, coating, bond layer and erodent) were created and implemented in the model. Coating response to an impact was quantified as the amplitude of the tensile peak in the surface of the coating. Stress field was tensile at the surface of the coating and compressive at the site of impact and also at the coating-substrate. These results were in accordance with the experimental results [8], [11].The coating internal structure (coating thickness, bond layer role thickness) and Young's modulus of coating is optimized from the point of view of maximum reduction in the tensile stresses in the surface. The approach used in this work is based on the modelling of stress distribution. In this context, minimum erosion rate will be obtained by minimizing tensile stresses that are responsible for crack initiation and propagation in the coating and the coating/substrate interface [8].

2 .Governing equation

The momentum equation below is governing equation [1]

$$M\ddot{U} = F^{ext} - F^{\text{int}} \quad \text{.....(1)}$$

Where M is the lumped mass matrix, $\ddot{U}$ is the nodal acceleration at each time step, F^{ext} is the externally applied load for each node and F^{int} is the internal force. This set of equations was solved using explicit time integration with the central difference method employing a lumped mass matrix, which improves the computational efficiency considerably. In our model, external force (F^{ext}) is zero while internal force (F^{int}) is generated due to impact of particle on coating surface.

3. Methodology of finite element analysis

3D model of a single particle impacting a monolayer coating with a bond layer on a steel substrate was developed using finite element method.

ABAQUS/CAE Student Edition 6.5-3 was used for model preparation whereas **ABAQUS/Explicit Student Edition 6.5-3** was used for calculations. The processing of the results was done using **ABAQUS/Viewer Student Edition 6.5-3.**

3.1 Materials modelled

Four types of materials were implemented in the models. They are Substrate, Coating, bond layer and eroding particle.

3.2 The Substrate was **PH-17 Stainless Steel** modelled as deformable elastic- plastic strain hardening material [10]. Its chemical composition (weight %) is Fe 73.7, Cr 17.5, Ni 3.8, Cu 2.9, Si 1.2, Mn 0.6and C 0.3. Its mechanical properties are Density 7810 kg/m^3, Young's modulus 196 GPa, Poisson's ratio 0.27, Yield strength 1208 MPa.

3.3 The coating was assumed to be **hard ceramic coating of TiN** [10]. To deposit the coating CVD methodology is used. It was modelled as elastic material with properties as Density 5220 kg/m^3, Young's modulus 200-600GPa, Poisson's ratio 0.25.

3.4 The bond layer, located between the coating and the substrate, was modelled as a **Titanium (Ti) layer** with deformable elastic-plastic properties. Properties of bond layer of TI are as density 5000 kg/m^3, Young's modulus 100 GPa, Poisson's ratio 0.27 [19].

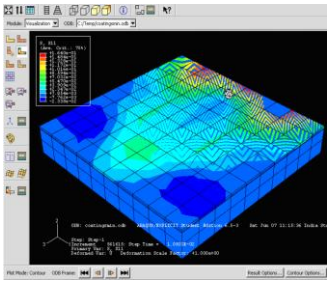

Fig. 1 Radial Stress Distribution with Coating thickness0.3mm, coating young's modulus 200 GPa and bond layer thickness 0.1mm

Figure 1 shows stress distribution on the surface

3.5 The Eroding Particle was modelled as a rigid sphere of **Alumina (Al_2O_3)** with radius 250 μm. Its mechanical properties are young's modulus 380 GPa, density 3950 Kg/m^3 and Poisson's ratio 0.22 [7].

3.6 Dimensions of the Model

The dimension of the substrate was $30\text{mm} \times 30\text{mm} \times 3\text{mm}$

The coating is $30\text{mm} \times 30$ mm with coating thickness varies from 0.3mm to 0.7 mm in steps of 0.2mm.

The bond layer of thickness 0.1mm, 0.2mm and 0.3mm is used.

The Al_2O_3 erodent was a spherical particle of 250 μm radius.

The dimensions of model parts and particle velocity were representative of the erosion conditions used in accelerated tests performed according to a standard procedure ASTM G76.

4. Results and discussion

Several 3-D FE models were prepared to perform calculations of the stresses in the coating. Simulations were performed with varied coating thickness, bond layer thickness and coating material properties. Substrate and eroding particle properties, dimensions and were kept constant in all simulations. A constant initial velocity of eroding particle of 100 m/s was used in all calculations.

4.1. RESULTS

A tensile stress peak (radial component) in the coating surface was selected as an optimization (damage controlling) parameter.

4.1.1 Effect of coating thickness

of the coating after the impact of the spherical particle. Coating thickness is 0.3 mm, bond layer thickness 0.1mm and coatings young's modulus was kept at 200 Gpa. Peak stress values as shown by the colour code are calculated. Also it can be seen that stress is compressive under impact and is tensile at away from impact point.

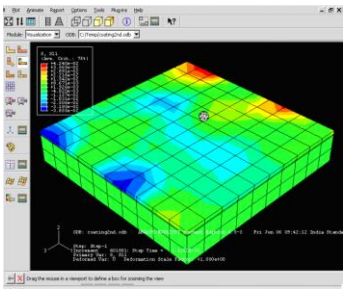

Fig. 2 Radial Stress Distribution with Coating thickness 0.5 mm, coatings young's modulus 200 GPa and bond layer thickness 01 mm

Figure 2 shows stress distribution on the surface of the coating after the impact of the spherical particle. Coating thickness is 0.5 mm, bond layer thickness 0.1mm and coatings young's modulus was kept at 200 GPa.

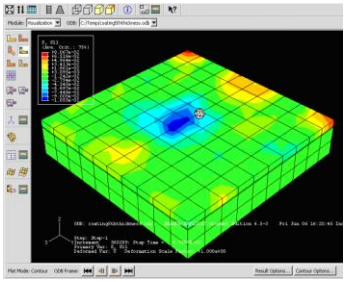

Fig. 3 Radial Stress Distribution with Coating thickness 0.7mm, coatings young's modulus 200 GPa and bond layer thickness 0.1mm

Figure 3 shows stress distribution on the surface of the coating after the impact of the spherical particle. Coating thickness is 0.7 mm, bond layer thickness 0.1mm and coatings young's modulus was kept at 200 GPa.

4.1.2 Effect of coating modulus

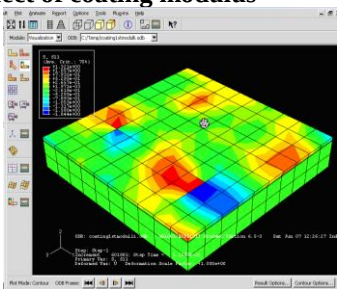

Fig. 4 Radial Stress Distribution with Coating thicknes0.3mm
coatings younng's modulus 300 GPa and bond layer thickness 0.1 mm

Figure 4 shows stress distribution on the surface of the coating after the impact of the spherical particle. Coating thickness was 0.3 mm, bond layer thickness 0.1mm and coatings young's modulus was kept at 300 GPa.

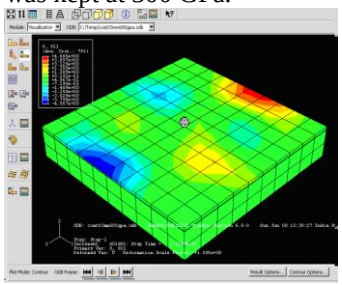

Fig. 5 Radial Stress Distribution with Coating thickness 3mm, Young's modulus 600 GPa and bond layer thickness 0.1mm

Figure 5 shows stress distribution on the surface of the coating after the impact of the spherical particle.

4.1.2.2 Coating thickness 0.7 mm with variation in Young's modulus

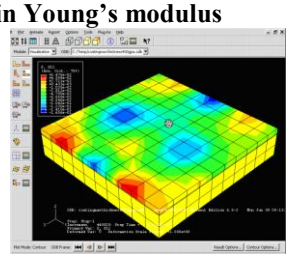

Fig. 6 Radial Stress Distribution with Coating thickness 0.7mm, Coatings young's modulus 400 GPa and bond layer thickness 0.1mm

In figure 6 Coating thicknesses was 0.7 mm, bond layer thickness 0.1mm and coatings young's modulus 400 Gpa. Maximum stress level increases.

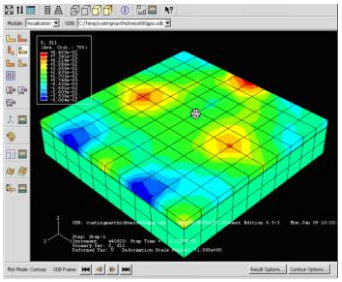

Fig. 7 Radial Stress Distribution with Coating thickness 0.7mm, coatings
young's modulus 600 GPa and bond layer thickness 0.1mm

Figure 7 shows stress distribution on the surface of the coating after the impact of the spherical particle. Coating thickness is 0.7 mm, bond layer thickness 0.1mm and coatings young's modulus

was kept at 600 GPa.

4.1.3 Bond layer thickness variation

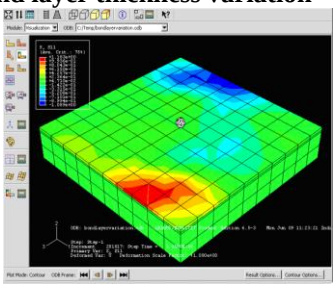

Fig. 8

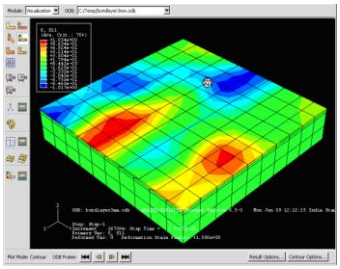

Fig. 9

Figure 8 and 9 shows effect of bond layer thickness variation on stress distribution.
In figure 8 coating thickness is 0.3 mm, bond layer thickness 0.2 mm and coatings young's modulus was kept at 200 Gpa. In figure 9 coating thickness is reduced to 0.2 mm and bond layer thickness was kept 0.3 mm and coatings young's modulus was 200 Gpa.

4.2 tables of radial stress (S11) value

Table 1 Effect of coating thickness variation on stress level with E_c = 200GPa

Coating thickness varies from 0.3 mm to 0.7 mm with bond layer, substrate properties are constant			
Coating thickness (mm)	Radial stress (S_{11})		Max. Principle stress × 10^3 GPa
	Tensile (+ve) × 10^3 GPa	Compressive (-ve) × 10^3 GPa	
0.3	0.164	-0.0233	3.377
0.5	0.0424	-0.03855	1.694
0.7	0.00309	-0.1055	0.9366

Table 2. Effect of coating Young's Modulus variation on stress level with coating thickness fixed at 0.3mm

Coating young's modulus varies from 200GPa to 600GPa while all other parameters are kept constant with coating thickness0.3mm.			
Coating young's modulus(E) GPa	Radial stress (S_{11})		Max. Principle stress × 10^3 GPa
	Tensile (+ve) × 10^3 GPa	Compressive (-ve) × 10^3 GPa	
200	0.164	-0.0233	3.377
300	1.321	-1.844	6.698
600	4.666	-4.567	19.7

Table 3. Effect of coating Young's Modulus variation on stress level with coating thickness fixed at 0.7mm

Coating young's modulus varies from 200GPa to 600GPa while all other parameters are kept constant with coating thickness0.7mm.			
Coating young's modulus(E) GPa	Radial stress (S_{11})		Max. Principle stress × 10^3 GPa
	Tensile (+ve) × 10^3 GPa	Compressive(-ve) × 10^3 GPa	
200	0.00309	-0.1055	0.9366
400	0.06476	-0.1606	4.597
600	0.08469	-0.05064	3.70

4.3 Effect of coating thickness: Graph

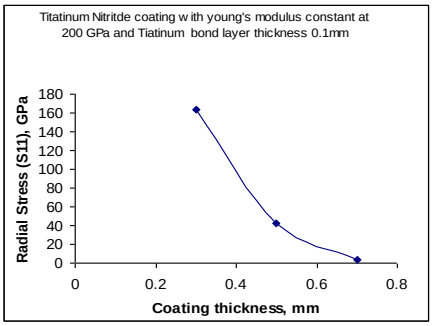

Fig. 10 Tensile Stress peak value vs. Coating Thickness

Figure 10 shows that the thicker the coating the lower the stress in the surface.

Bond layer thickness(mm)	Tensile stress S11(GPa)	Coating description
0.2 0.3	1183 1034	TiN coating with E=200 GPa , (total coating thickness=0.4mm)

Table 8 Effect of bond layer thickness

4.4 Effect of Coating Modulus: Graph

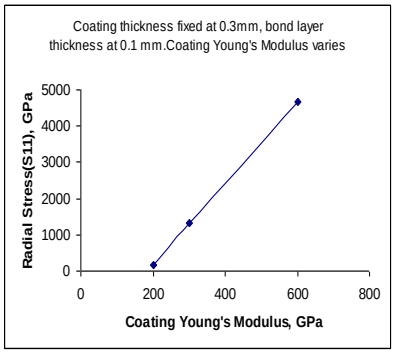

Fig. 11 Radial Stress (S11) vs. Coating Young's Modulus

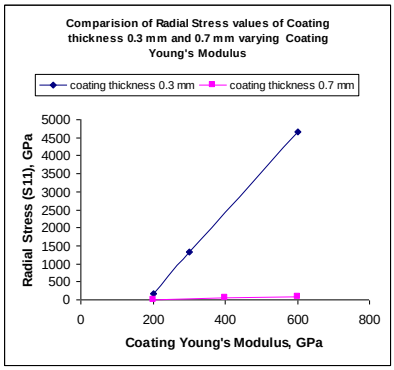

Fig. 12 Amplitude of radial tensile stress (S11) vs. Coating Modulus

Figure 11 shows that stress level on the surface of the coating is strongly dependent upon young's modulus of the coating.

4.5 Effect of Bond Layer

In coating technology, a very thin metallic bond layer (often chromium (Cr) or titanium (Ti)) is used to improve coating adhesion to the substrate. Bond layer thickness is varied from 0.2 mm to 0.3 mm. total coating thickness was kept 0.4 mm. It can be seen from table 8 that thick bond layer reduces the stress level. However the reduction is not very much.

4.6 Validation of the FE Model

The results of the proposed finite element model are compared with the experimentally obtained results of Nicholls et al (2004)

References

1. M.S.ELtobgy, E. Ng, M.A. Elbertawi, Finite Element modelling of erosive wear, Machine Tool and Manufacture 44 (2004) 1337-1346.

2. K.Shimizu, T. Noguchi, H. Seitoh, M. Okada, Y Matsubara, FEM analysis of erosive wear, Wear 240 (2001) 779-784.

3. P.J. Woytowitz, R.H. Richman, Modelling of damage from multiple impacts by spherical particles, Wear 233–234 (1999) 120–133.

4. I.M. Hutchings, R.E Winter, Particle Erosion of Ductile Metals: A Mechanism of Material Removal, Wear, 27 (1974) 121-128.

5. I. Finnie, Some reflections on past and future of erosion, Wear 186-187 (1994)1-10.

6. J. G. A. Bitter, A study of erosion phenomena part 1, Wear, 6 (1963) 4-21.

7. G. Sundararajan, The solid particle erosion of metallic materials: The rationalization of the influence of material variables, Wear186187 (1994)129-144.

8. S. Hassani, J.E. Klemberg-Sapieha, M. Bielawski. Design of hard coating architecture for the optimization of erosion resistance, Wear 264 (2008) 879–887.

9. J.R. Nicholls, D.J.Stphenson, Monte Carlo modelling of erosion processes, Wear 186- 187(1994) 64-77.

10. A. Leyland, A. Matthews, Thick Ti/TiN multilayered coatings for abrasive and erosive wear resistance, Surf. Coat. Technol. 70 (1994) 19–24.

11. J.R. Nicholls, D.J.Stphenson, Monte Carlo modellling of erosion processes, Wear 186- 187 (1994) 64-77.

12. Q. Chen, D.Y Li, Computer simulation of solid particle erosion, Wear 244(2003) 203-210.

13. D.Griffin et al., The development of three dimensional finite element model for solid particle erosion on an alumina scale/ MA946 substrate, Wear 246(2004)900-906.

14. Iain Finnie, Erosion of surfaces by solid particles, Wear, 3 (1960) 87-103.

15. A.G. Evans, Impact damage mechanics: solid projectiles:

C.M. Preece (Ed.),treatise on Materials Science and Technology, vol. 16 Erosion, Academic Press, NY, 1979, pp. 1–67.

16. Evaluation Of Two Tin Coatings Applied To Compressor Blades R. Berriche, P. Au, J-P. Immarigeon, Institute for Aerospace Research National Research Council of Canada Ottawa, Ontario, Canada Kl A OR6. M. Donaghy, Department of National Defense Ottawa, Ontario, Canada K 1 A OK2.

17. J.N.Reddy, an introduction to the Finite Element Method, 3rd edition, Tata McGraw- Hill, NY. ISBN-0-07-060741-9.

18. T.Z. Gorishnyy, L.G. Olson, M. Oden, S.M. Aouadi, S.L. Rohde, Optimization of wear-resistant coating architectures using finite element analysis, J. Vac. Sci. Technol. A 21 (2003) 332–339'

19. A. Leyland, A. Matthews, Thick Ti/TiN multilayered coatings for abrasive and erosive wear resistance, Surf. Coat. Technol. 70 (1994) 19–24.

20. Colin R. Gagg, Peter R. Lewis. Wear as a product failure mechanism- Overview and case studies. Engineering Failure Analysis 14 (2007) 1618–1640.

21. K. Bose, R.J.K. Wood, D.W. Wheeler, High energy solid particle erosion mechanism of superheated CVD coatings. Wear 249 (2004) 134–144.

22. 14. M. I. Darby, g. R. Evans, Department of Pure and Applied Physics, University f Salford, Salford, Lancs. M4 4WT (U.K.).

23. A. Hamed,W. Tabakoff, R.Wenglarz, Erosion and deposition in turbomachinery, J. Propul. Power 22 (2006) 340–360.

24. Denis Jelagin, Per-Lennart Larsson, Hertzian fracture at finite friction: A parametric study, Wear 264 (2008) 840–848.

25. D. Elaguine, M.-A. Brudieu, B. Stor°akers, Hertzian fracture at unloading, J. Mech. Phys. Solids 44 (2006) 2443–2473.

26. R. Lewis, A modelling technique for predicting compound impact wear, Wear 262 (2007) 1416–1421.

27. S.B. Mishra, K. Chandra, S. Prakash, B. Venkataraman, Characterisation and erosion behaviour of a plasma sprayed Ni3Al coating on a Fe-based superalloy, Materials Letters 49 (2004) 3694 – 3698.

28. Y.S. Zhang, K. Wang, Z. Han, G. Liu, Dry sliding wear behavior of copper with nano-scaled twins, Wear 262 (2007) 1463–1470.

29. M. Laribi, A.B. Vannes, D. Treheux, Study of mechanical behavior of molybdenum coating using sliding wear and impact tests, Wear 262 (2007) 1330–1336.